



# Assessing evapotranspiration in a lettuce crop with a two-source energy balance model

Ramesh Dhungel<sup>1</sup> · Ray G. Anderson<sup>1,2</sup> · Andrew N. French<sup>3</sup> · Mazin Saber<sup>4</sup> · Charles A. Sanchez<sup>5</sup> · Elia Scudiero<sup>1,2</sup>

Received: 24 April 2022 / Accepted: 4 August 2022 / Published online: 26 August 2022

This is a U.S. Government work and not under copyright protection in the US; foreign copyright protection may apply 2022

## Abstract

Winter vegetables, including lettuce, are a significant consumptive use of water in the Lower Colorado River Basin. Precise irrigation management is needed to increase water use efficiency and reduce the negative impacts of suboptimal irrigation, including nutrient leaching, crop stress, and crop pathogens. However, lettuce has multiple features that make accurate evapotranspiration (ET) modeling difficult, including asynchronicity with meteorological evaporative demand, short growing seasons, and a shallow root zone that increases the risk of using an incorrect ET value. To improve ET modeling and understand applied irrigation effectiveness for lettuce in this region, we used an energy and water balance bio-physical model, Backward-Averaged Iterative Two-Source Surface temperature and energy balance Solution (BAITSSS) on arid farmlands in the lower Colorado River basin. The study was conducted between 2016 and 2020 at twelve eddy covariance (EC) sites in lettuce with a wide range of soil physical properties. BAITSSS was implemented using ground-based weather and irrigation data, and remote sensing-based vegetation indices (Sentinel-2). The model accuracy varied among sites, with a mean cumulative seasonal ET of ~3% and mean RMSE of 1.1 mm d<sup>-1</sup> when compared to EC. The results showed that accurate timing and amount of applied water (irrigation and precipitation) were critical to capturing ET spikes right after irrigation and tracking the continuous decrease of ET. This study highlighted the dominant factors that influence the ET of lettuce and how BAITSSS can improve ET modeling for irrigation management.

## Introduction

The Colorado River supplies vital irrigation water for Yuma County, Arizona, which is one of the world's leading producers of lettuce and other winter vegetables (French et al. 2020). This low desert region is fully dependent on irrigation for crop production (Sanchez et al. 2009). However,

the prolonged drought in California and the Western United States had a significant adverse effect on irrigated agriculture (Lund et al. 2018; Chikamoto et al. 2020), where these effects were also propagated to the Colorado River Basin (Sanchez et al. 2009; Chikamoto et al. 2020; Norton et al. 2021). Therefore, efficient irrigation is critical for managing the scarce water resources in this region (Sanchez et al. 2009).

One way to achieve efficient irrigation practice is to estimate evapotranspiration (ET) using thermal remote sensing-based energy balance models (Melton et al. 2012, 2021; Kilic et al. 2016; Fisher et al. 2017; Anderson et al. 2021). These models make it possible to assess instantaneous crop water use and diagnose crop water stress. However, integration of irrigation, critical to efficient water management of the agriculture sector (Melton et al. 2012), is largely unaccounted for due to the lack of these data (Alexandridis et al. 2014) and the lack of water balance components in the energy balance models. These thermal-based models rely on instantaneous thermal images that are not always available at desired temporal and spatial resolutions and which are frequently obscured by clouds (Long and Singh

✉ Ramesh Dhungel  
ramesh.dhungel@usda.gov

<sup>1</sup> USDA-Agricultural Research Service (ARS), US Salinity Laboratory, Agricultural Water Efficiency and Salinity Research Unit, Riverside, CA 92507, USA

<sup>2</sup> Riverside, Department of Environmental Sciences, University of California, 900 University Ave, Riverside, CA 92521, USA

<sup>3</sup> USDA-ARS, US Arid Land Agricultural Research Center, 21881 N. Caardon Ln, Maricopa, AZ 85138, USA

<sup>4</sup> University of Arizona, Yuma Agricultural Center, 6425 W 8th St, Yuma, AZ 85364, USA

<sup>5</sup> University of Arizona, Maricopa Agricultural Center, 37860 W Smith Enke Rd, Maricopa, AZ 85138, USA

2010; He et al. 2017; Anderson et al. 2021). The resulting time gap between two clear thermal satellite images and the alteration of surface temperatures by recent irrigation or precipitation events further confounds and adds uncertainty in ET modeling.

To overcome difficulties integrating ET and irrigation, a remote-sensing-based two-source surface energy balance (Backward-Averaged Iterative Two-Source Surface temperature and energy balance Solution; BAITSSS) was developed to incorporate soil water components within an energy balance framework (Dhungel et al. 2016, 2019a, 2021). BAITSSS estimates surface temperature internally in the energy balance based on the weather, vegetation indices, vegetation physical properties, and soil moisture conditions for each time step. Soil water from the root zone in BAITSSS was integrated using the Jarvis-type canopy resistance scheme (Jarvis 1976). BAITSSS needs information related to field-scale irrigation ( $I_{rr}$ ) and precipitation ( $P$ ) for soil water balance. BAITSSS uses either measured or estimated  $I_{rr}$  based on soil hydraulic characteristics [soil moisture at field capacity ( $\theta_{fc}$ ) and wilting point ( $\theta_{wp}$ )], and management allowed depletion (MAD). However, the water balance approach is also subject to uncertainty and challenges such as correct characterization of soil physical properties, stomatal response to environmental factors [either through Jarvis or Ball–Berry–Leuning model types (Ball et al. 1987; Leuning 1990, 1995)], rooting depth, and prior knowledge of field-scale irrigation timing and amount. Challenges remain to estimate accurate timing and the amount of applied  $I_{rr}$  on a landscape scale by remote sensing techniques (Massari et al. 2021). The estimated  $I_{rr}$  may not always concur with the applied  $I_{rr}$  in the field.

In previous work, the BAITSSS model was evaluated to lysimeter ET observations of corn and sorghum in an advective environment of Bushland, Texas (Dhungel et al. 2019a, 2021). These studies showed the advantages of the energy balance model with water balance components for capturing the wetting and drying events from irrigation and precipitation for precise hourly, daily, and seasonal ET estimation. However, the phenology and growing period of winter lettuce differ from corn/sorghum, thus requiring further model evaluation. Some specific challenges for ET modeling of lettuce are shallow root depth compared to grain crops (Escarabajal-Henarejos et al. 2015), short growing seasons (Thorup-Kristensen 2001; Roux et al. 2016), and longer partial cover period. In most environmental conditions, full canopy cover coincides with peak reference ET. There is relatively less uncertainty in ET with an un-stressed full canopy cover crop, whereas there is greater uncertainty under partial cover coinciding with the initial stage and at the end-season (Kc  $_{ini}$  and Kc  $_{end}$ , where Kc is crop coefficient). With winter crop production, we have a situation where reference ET is highest during Kc  $_{ini}$  and Kc  $_{end}$ , so there is greater relative

uncertainty. Furthermore, the timing of vegetative growth and meteorological demand is out phase for winter lettuce production in Yuma and other low desert regions.

Some of the earlier studies related to lettuce ET in the western United States were Johnson et al. (2016) in Salinas, California, and Johnson and Trout (2012) in California's San Joaquin Valley. In these studies, Johnson and colleagues utilized the FAO-56 Penman–Monteith reference ET model (Allen et al. 1998, 2005b) and normalized difference vegetation indices (NDVI)-crop coefficients to calculate ET. To our knowledge, the study of seasonal ET using remote sensing (Sentinel-2) based energy balance model for lettuce at the Lower Colorado River basin, has not been conducted. The overall objective of this study was to evaluate the ET of lettuce under well-watered conditions and to understand the dominant factors and challenges. Other questions we investigated were the influence of soil hydraulic characteristics in irrigation effectiveness and to final ET.

## Materials and methods

### Study area and evapotranspiration observations

The study area is in the Lower Colorado River Basin in Yuma County, Arizona. Elevation of Yuma Valley ranges from 24 to 44 m. Lettuce (September through January of next year) is one of the major cultivated crops of the Colorado River Basin in the USA (Berardy and Chester 2017; Frisvold et al. 2018). The study area receives minimal precipitation ( $\sim 80 \text{ mmy}^{-1}$ ) (Arguez et al. 2010) with irrigation supplied by the Colorado River. The study sites use sprinkler and furrow irrigation and are well watered. Both irrigation types are frequently adopted in the same site and season for lettuce cultivation. Sprinklers are used during crop establishment to create a cool microclimate and to help with crop establishment. Sprinklers are usually discontinued in  $\sim 14$  days, with furrow irrigation used thereafter (Sanchez et al. 2009).

Twelve EC sites (within the range of  $600 \text{ km}^2$ ) between 2016 and 2020 were used to evaluate model simulated ET (Table 1). The EC site deployments were similar to those described in French et al. (2020). System components comprised sonic anemometers from Campbell Scientific (Logan, UT), infrared gas analyzers from LICOR (Lincoln, NE), net radiometers from Kipp & Zonen (Delft, Netherlands), soil heat flux plates from Hukseflux (Delft, Netherlands), and air temperature and humidity probes from Vaisala (Helsinki, Finland). Loggers and covariance sensors were calibrated by the manufacturer in 2016 and 2017. Zero and span of infrared gas analyzers (IRGA) were done in July 2017 and again in July 2018.

**Table 1** Site locations, crop season, soil hydraulic characteristics, and year of lettuce for various sites over multiple years (2016–2020) at Colorado River Basin region

SN	Site	Input data source for BAITSSS	Season	Season length (days)	Latitude	Longitude	Field capacity $\text{m}^3 \text{m}^{-3}$	Available water capacity $\text{m}^3 \text{m}^{-3}$	Difference between applied water ( $P + I_r$ ) and ET from EC %
a	NGIDD 19-20a	EC	2019–2020	93	32.7485	–114.5077	0.19	0.18	7.8
b	YID 18b	EC	2018–2019	87	32.6967	–114.5375	0.32	0.20	15.4
c	YCWUA 18a	EC	2018	68	32.6562	–114.6564	0.42	0.16	43.6
d	YID 17a	EC	2017	63	32.6974	–114.5195	0.30	0.20	–4.9
e	YID 19-20a	AZMET	2019–2020	100	32.7091	–114.5227	0.19	0.18	39.7
f	YCWUA 19-20a	AZMET	2019	74	32.5801	–114.7332	0.42	0.16	41.6
g	YID 17d	AZMET	2017	84	32.6972	–114.5154	0.30	0.20	11.8
h	YID 17b	AZMET	2017	75	32.6973	–114.5238	0.30	0.20	7.0
i	YID 17c	AZMET	2017	70	32.6972	–114.5280	0.32	0.20	–9.5
j	YCWUA 17-18b	AZMET	2017–2018	107	32.7065	–114.7079	0.32	0.20	26.8
k	YCWUA 17-18a	AZMET	2017–2018	97	32.7207	–114.7059	0.42	0.16	30.6
l	YID 16	AZMET	2016	64	32.6935	–114.5142	0.32	0.20	21.2

Four out of twelve sites had complete weather data available at EC sites as indicated

SN Figure Panel, EC Eddy Covariance, AZMET Arizona Meteorological Network, NGIDD North Gila Valley Irrigation and Drainage District, YID Yuma Irrigation District, YCWUA Yuma County Water Users' Association

Each station collected micrometeorological observations (~108 variables per time step) at 20 Hz, configured under Campbell Scientific's EasyFlux DL™ (Logan, UT) program<sup>1</sup> to allow continuous data measurements during the cropping cycle. Simultaneously 30-min block-averaged fluxes, including the Webb–Pearman–Leuning (Webb et al. 1980) corrections were stored.

Raw data were processed with EddyPro software in Express Mode (Fratini and Mauder 2014). Changes in energy storage within the soil mass above the two heat flux plates were computed. Data spike removal followed the outlined methodology described by Vickers and Mahrt (1997). The online gap-filling tool (<http://www.bgc-jena.mpg.de/~MDIwork/eddyproc/method.php>; employing techniques as described in Falge et al. (2001) and Reichstein et al. (2005) were used to fill time gaps including those when the friction velocity ( $U^*$ ) was less than  $0.15 \text{ ms}^{-1}$ . Assessment of energy balance closure was done at daily time steps by regressing advective energy against radiative energy and correcting for net energy storage via photosynthesis (Anderson and Wang 2014). Energy balance closure was enforced at 30-min time steps by assigning residuals to latent heat (LE) fluxes (Rosa and Tanny 2015). Two-dimensional flux footprint analyses were done using an R script provided by Kljun et al. (2015).

<sup>1</sup> Mention of trade names or commercial products in this publication is solely for the purpose of providing specific information and does not imply recommendation or endorsement by the U.S. Department of Agriculture.

With minor exceptions, 80% of the flux footprints lay within plot boundaries. Daily fluxes were computed by summing the 30-min LE flux values. Full details about the EC data and processing will be presented in a forthcoming paper (French et al. in prep.).

### BAITSSS model

BAITSSS model is comprised of energy and soil water balance components connected in a series-resistance network (Fig. 1). The full details of the BAITSSS model and equations can be found in Dhungel et al. (2016, 2019a, b). Here, we present a summary and equations of the model. BAITSSS couples these resistances with an aerodynamic equation to compute latent and sensible heat flux. It adopts the Jarvis scheme (Eq. 1) for estimating canopy resistance ( $r_{sc}$ ) while soil surface resistance ( $r_{ss}$ ) is estimated empirically using soil moisture at the surface ( $\theta_{sur}$ ) and saturation ( $\theta_{sat}$ ) (Shu 1982) (Eq. 2). The Jarvis-type  $r_{sc}$  scheme considers weighting functions representing plant response to incoming solar radiation ( $F_1$ ), air temperature ( $F_2$ ), vapor pressure deficit ( $F_3$ ), and soil moisture in the root zone ( $F_4$ ). These weighting functions vary from 0 to 1 with a minimum canopy resistance ( $r_{sc}$ ) of  $40 \text{ m s}^{-1}$  and maximum resistance of  $5000 \text{ ms}^{-1}$ . BAITSSS does not utilize FAO-56 reference ET ( $ET_0$ ) to constrain maximum ET, however, it limits the values of resistances i.e.,  $r_{ss}$  and  $r_{sc}$ . The minimum  $r_{sc}$  ( $R_{c\_min}$ ) was set to  $40 \text{ sm}^{-1}$  for irrigated agriculture (Lhomme et al. 1998; Kumar et al. 2011; Zhang et al. 2014; Dhungel et al. 2019a) and the

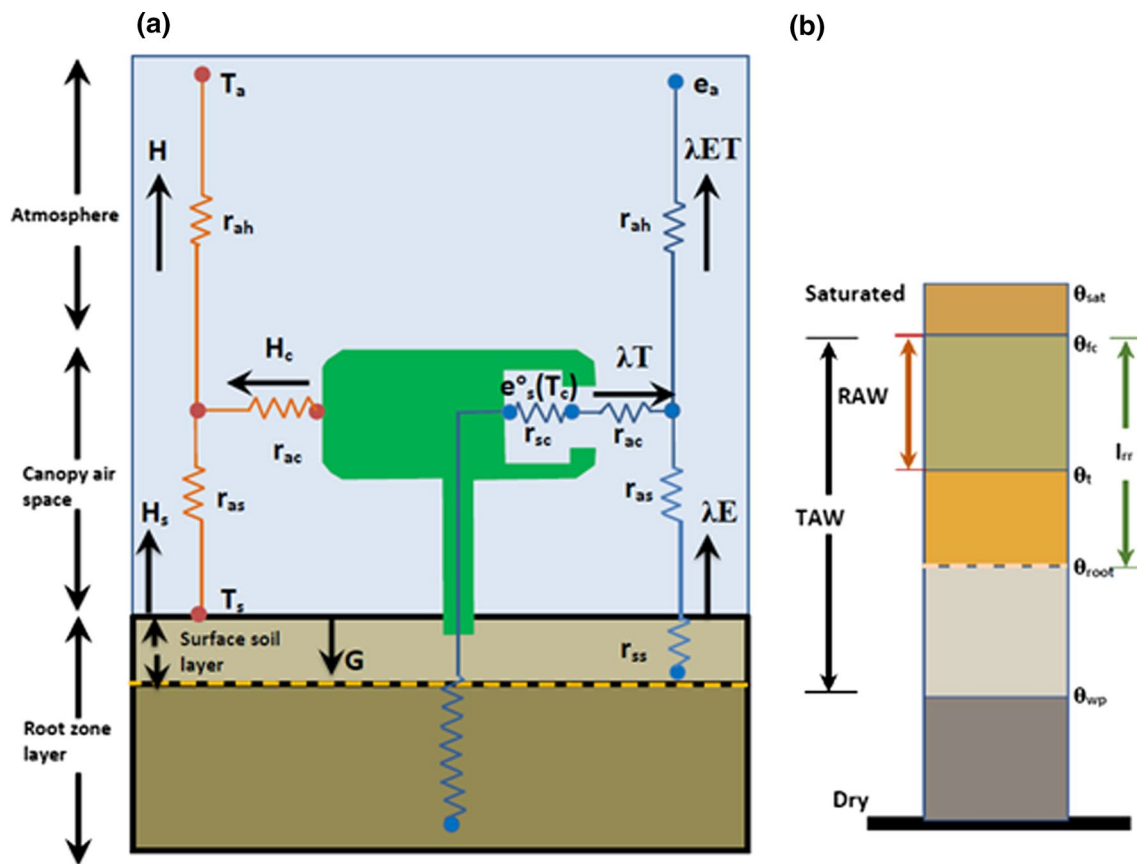


**Fig. 1** The BAITSSS simulation energy balance scheme (a), models energy fluxes between plants (green), soil (brown), and air (light blue) components using two resistance networks, one for sensible heat ( $H$ , orange), another for latent heat ( $\lambda E$ , blue), each connected to soil heat flux elements ( $G$ , black). s and c subscripts, respectively, denote for soil and canopy components. The soil water balance scheme includes a representation of soil water status (b). Symbols include: evaporation ( $E$ ), transpiration ( $T$ ), latent heat of vaporization ( $\lambda$ ), air temperature ( $T_a$ ), soil surface temperature ( $T_s$ ), canopy

temperature ( $T_c$ ), aerodynamic resistance ( $r_{ah}$ ), soil surface resistance ( $r_{ss}$ ), canopy resistance ( $r_{sc}$ ), aerodynamic resistance between the substrate and canopy height ( $r_{as}$ ), bulk boundary layer resistance of vegetative elements in the canopy ( $r_{ac}$ ), volumetric moisture content at saturation ( $\theta_{sat}$ ), volumetric water content at field capacity ( $\theta_{fc}$ ), volumetric water content at root zone ( $\theta_{root}$ ), volumetric water content at wilting point ( $\theta_{wp}$ ), readily available water (RAW), and total available water (TAW) (color figure online)

minimum value of  $r_{ss}$  to  $35 \text{ sm}^{-1}$ . BAITSSS and a similar two-source energy balance model (Anderson et al. 2007) use a logistic equation to calculate the effects of the available water fraction (AWF) on  $F_4$  where AWF is computed based on  $\theta_{fc}$  and  $\theta_{wp}$ . These curves are used to define the points and periods of moisture-related stress to vegetation. Soil hydraulic characteristics play an important role to capture this non-linear process. Leaf area index (LAI) is rescaled by the fraction of canopy cover ( $f_c$ ), i.e.,  $\text{LAI } f_c^{-1}$  (Bohn and Vivoni 2016; Dhungel et al. 2019a). While these canopy characteristics are partially correlated, this scaling approach was found to more accurately account during partial cover period provided by the emergent canopy than using LAI alone. As the canopy approached full closure, effects of this adjustment diminish, and the original relationship is maintained as  $f_c$  values approach unity (Dhungel et al. 2019a).

$$r_{sc} = \frac{R_{c\_min}}{\frac{\text{LAI}}{f_c} F_1 F_2 F_3 F_4}, \quad (1)$$

$$r_{ss} = 3.5 \left( \frac{\theta_{sat}}{\theta_{sur}} \right)^{2.3} + 33.5. \quad (2)$$

Irrigation in BAITSSS is applied when root zone moisture ( $\theta_{root}$ ) reaches a threshold moisture content. The threshold moisture content is computed from soil hydraulic characteristics ( $\theta_{fc}$ ,  $\theta_{wp}$ ). In this study, actual irrigation data were available and, thus, utilized by BAITSSS. BAITSSS differentiates irrigation as either applying water to both layers (soil layer and root zone) with sprinklers or furrow irrigation or only in the root zone as a sub-surface drip. None of the fields in this study used sub-surface

**Table 2** Water balance components of lettuce for various sites over multiple years (2016–2020) at Colorado River Basin region

SN	Site	Irrigation mm	Precipitation mm	ET from EC mm	ET from BAITSSS mm	NDVI < 0.3		NDVI ≥ 0.3	
						r <sup>2</sup>	RMSE	r <sup>2</sup>	RMSE
a	NGIDD 19-20a	308.6	32.3	314.1	270.1	0.67	0.97	0.46	0.80
b	YID 18b	274.2	17.8	247.0	259.9	0.26	1.31	0.64	0.53
c	YCWUA 18a	442.9	24.1	263.2	260.6	0.77	0.94	0.71	0.79
d	YID 17a	257.0	0.0	269.7	251.6	0.38	1.43	0.45	1.27
e	YID 19-20a	435.1	58.1	297.5	315.2	0.40	1.03	0.69	0.91
f	YCWUA 19-20a	406.8	34.3	257.4	267.7	0.54	1.23	0.73	0.83
g	YID 17d	281.2	1.3	249.0	263.5	0.32	1.90	0.56	0.93
h	YID 17b	328.6	1.3	306.9	296.8	0.47	1.70	0.38	1.29
i	YID 17c	243.1	1.3	267.6	232.8	0.69	1.13	0.08	1.25
j	YCWUA 17-18b	411.5	2.0	302.8	381.0	0.36	1.13	0.42	1.44
k	YCWUA 17-18a	335.3	2.0	234.1	285.2	0.76	0.79	0.08	1.46
l	YID 16	310.3	1.3	245.6	257.6	0.47	1.27	0.44	0.99

Statistics depending on the NDVI range (<0.3, ≥0.3) were also shown. Data are reported for each cropping season, which varied in length

drip. With one exception (YID 17a), fields were irrigated through a sprinkler for the establishment and thereafter through furrow irrigation, and irrigation water was applied evenly to both layers for the entire root depth. A constant value of  $0.45 \text{ m}^3 \text{ m}^{-3}$  was used for  $\theta_{\text{sat}}$  in all sites. The albedo was set to 0.2 for bare soil and to 0.15 for vegetation (Dhungel et al. 2019a).

Hourly weather data (solar radiation, air temperature, relative humidity, and wind speed) were acquired from both the Yuma Valley station of the Arizona Meteorological Network (AZMET, [cals.arizona.edu/AZMET](http://cals.arizona.edu/AZMET)) (coordinates  $32.709828^\circ \text{ N}$ ,  $114.707521^\circ \text{ W}$ , and 36 m above sea level) and the EC stations. Four out of twelve sites had complete weather data available at EC sites while the rest of them were from AZMET (Table 1). AZMET data were used to supplement EC sites that only had a net radiometer and that lacked solar irradiance observations. The measurement height of weather data was 2 m for AZMET and 3 m for the EC site and applied accordingly while executing the model. Simulations from BAITSSS were carried out for hourly timesteps and later accumulated to a daily scale for comparison purposes. We chose to compare BAITSSS and EC at daily time scales because EC suffers energy imbalance and evapotranspiration hysteresis due to failure to account for heat and energy storage in an hourly timescale (Leuning et al. 2012; Dhungel et al. 2021); however, imbalance may not be completely eliminated to daily scale.

A soil surface depth of 150 mm (Allen et al. 2005a) and rooting depth of 500 mm for lettuce (Frisvold et al. 2018) were prescribed for the model for the entire simulation period. The simulation periods (planting to harvesting) varied for each of these sites, with the earliest and latest planting being September 13th [Day of year (DOY) 256] and November 19th

(DOY 323), respectively. The minimum and maximum simulation periods were 63 days and 107 days (Table 1).

We estimated fractional canopy cover ( $f_c$ ) from surface reflectance L2A Sentinel-2 data converted to normalized difference vegetation indices (NDVI) (Gutman and Ignatov 1998). Further, the leaf area index (LAI) was estimated from NDVI using an empirical equation as no measured values were available.

$$f_c = \frac{\text{NDVI} - \text{NDVI}_{\min}}{\text{NDVI}_{\max} - \text{NDVI}_{\min}} \quad (3)$$

We adopted area and depth-averaged soil hydraulic characteristics (field capacity and available water capacity) based on the Soil Survey Geographic database SSURGO as described by Wicczorek (2014) (Table 2). The study sites showed large variations of soil hydraulic characteristics, with  $\theta_{fc}$  ranging between 0.19 and  $0.42 \text{ m}^3 \text{ m}^{-3}$  and available water content ( $\theta_{\text{awc}}$ ) between 0.10 and  $0.20 \text{ m}^3 \text{ m}^{-3}$ .

One of the challenges of soil water balance models like BAITSSS is to estimate reasonable initial soil moisture conditions when no measured data are available. Data showed that irrigation was mostly applied for the first day after planting followed by multiple small irrigation events (<20 mm) during initial planting period in all sites. Analysis during the last 15 days before the start of the simulation revealed that most sites received no precipitation (P), with the remainder receiving less than 15 mm. Therefore, a relatively dry soil profile of  $0.01 \text{ m}^3 \text{ m}^{-3}$  at the surface (150 mm) and residual moisture of wilting point moisture content ( $\theta_{\text{wp}}$ ) at the root zone were adopted as initial conditions for all sites.

We evaluated the impact of initial boundary conditions and input parameters, i.e., (a) initial soil moisture conditions, (b) soil surface and root zone depth, (c) soil hydraulic

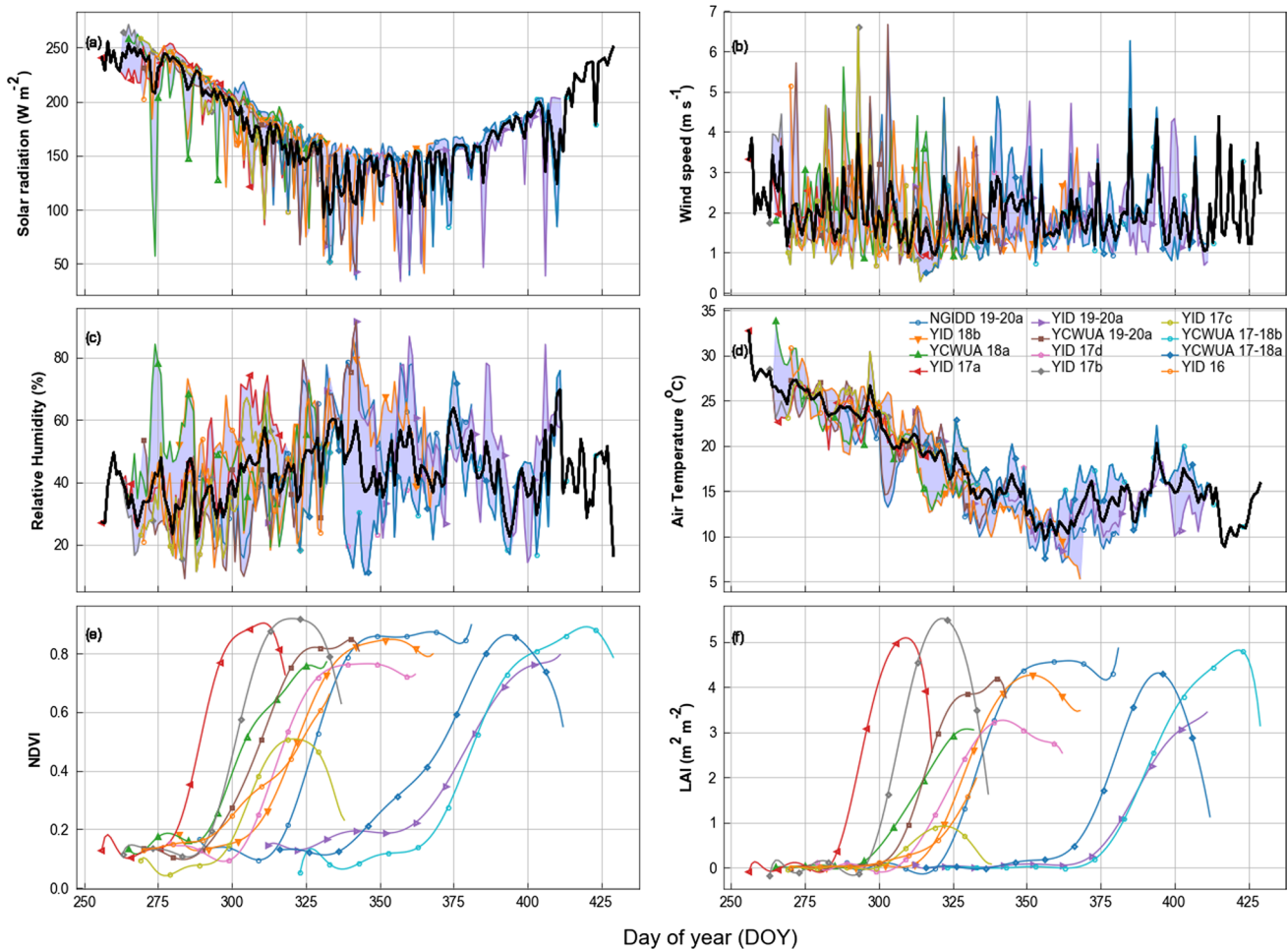


**Fig. 2** Daily mean weather variables (incoming solar radiation, wind speed, relative humidity, air temperature), and normalized difference vegetation index (NDVI) and leaf area index (LAI) of lettuce for vari-

ous sites over multiple years (2016–2020) at Colorado River Basin region. Mean values of weather variables among years and sites are shown in thick black color (color figure online)

characteristics ( $\theta_{awc}$ ,  $\theta_{fc}$ , and  $\theta_{wp}$ ), (d) vegetation indices (NDVI), canopy physical properties (LAI), and (e) weather data (AZMET vs. EC) in BAITSSS and then ET outputs were compared with observed EC. Parameters with potential for larger uncertainties (e.g., soil surface and root zone depth, initial soil moistures) were varied from lower to upper values with  $\sim 20\%$  increase in each simulation. We also evaluated assumptions of identical soil hydraulic characteristics (for instance,  $\theta_{fc} = 0.32$  and  $\theta_{awc} = 0.32$  to all sites).

## Results and discussion

### Weather and vegetation indices

Seasonal variation of meteorological variables, vegetation indices, and canopy physical properties are shown in Fig. 2. As expected, solar radiation and air temperature decreased towards winter solstice and increased afterward

into the new calendar year (Fig. 2a and d). Relative humidity and wind speed showed dissimilar behavior, with lower relative humidity positively correlated with higher wind speed (Fig. 2b and c). At the start of the simulation, average flux (diurnal cycle; 24 h) of solar radiation among the sites was  $\sim 250 \text{ Wm}^{-2}$ , while at the end of the year was  $\sim 150 \text{ Wm}^{-2}$ . Similarly, the daily mean air temperature decreased from  $\sim 30^\circ \text{C}$  to  $\sim 10^\circ \text{C}$  during that period. Daily mean maximum observed values of solar radiation, wind speed, relative humidity, and air temperature were  $271 \text{ Wm}^{-2}$ ,  $7 \text{ ms}^{-1}$ ,  $92\%$ , and  $34^\circ \text{C}$ , respectively, among sites and years. Variations in NDVI and LAI among sites may be due to differences in planting densities. Some sites show a marginal decrease in vegetation indices after the peak vegetative cover, while the majority did not. Out of all fields, YID 17c had the lowest value of NDVI and LAI (Fig. 2e and f) and also showed a significant decrease after the NDVI peak. Lettuce crops are harvested at peak or close to peak vegetative cover; thus, a decrease in NDVI after peak is mostly due to the harvest

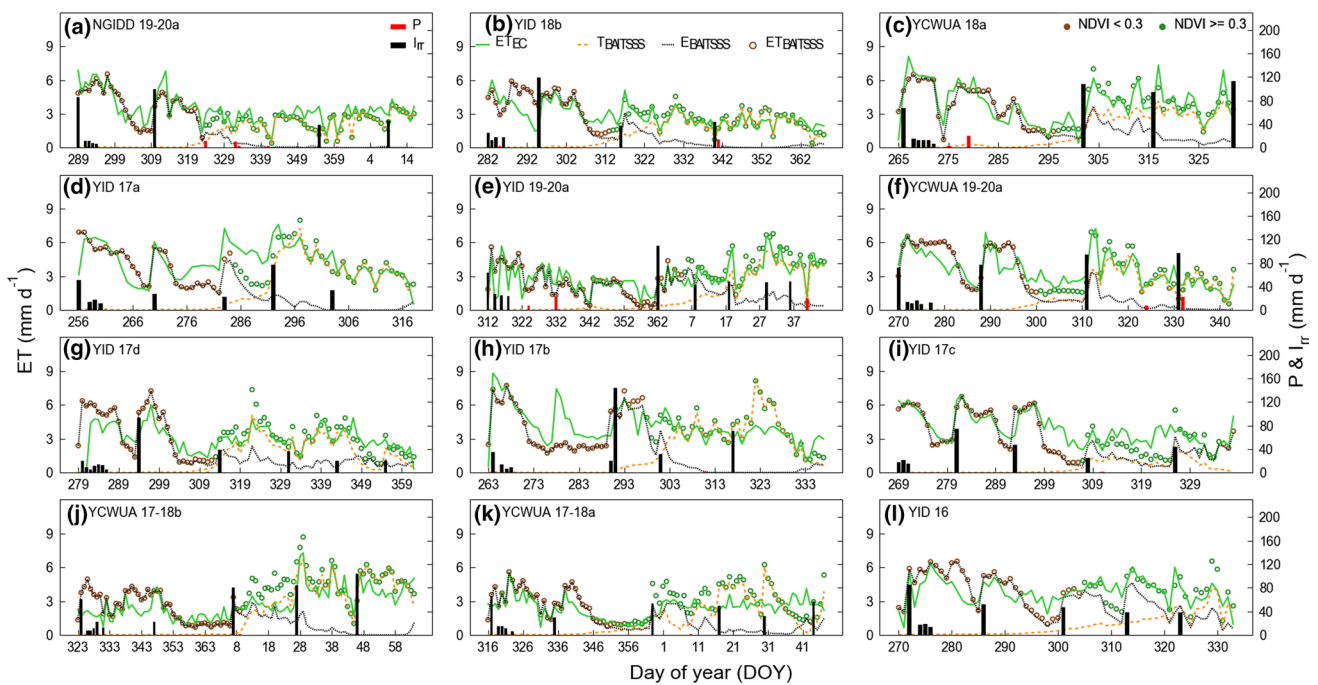


**Fig. 3** Comparison of daily evapotranspiration (ET, green or brown), evaporation (E, black), transpiration (T, orange) from BAITSSS, eddy covariance (EC), applied irrigation ( $I_{rr}$ , black), and precipitation (P,

red) of lettuce for various sites over multiple years (2016–2020) at Colorado River Basin region. ET varying on NDVI values indicated by symbol color (color figure online)

activities. The NDVI and LAI peaked during the same year as planting except for the last crops (Fig. 2e and f). The maximum value of NDVI and LAI were 0.92 and  $5.5 \text{ m}^{-2}$ , respectively. The NDVI and LAI values were smoothed with a 7-day convolution filter to reduce daily scatter. While solar radiation and air temperature mainly were decreasing, vegetation indices were increasing except for the late-planted ones. The mean P during the simulation period among the sites was 15 mm, while the mean  $I_{rr}$  was 343 mm. Seven out of twelve sites received less than 5 mm precipitation during the entire simulation period (Table 2).

### Evapotranspiration time series

The ET time series plot showed BAITSSS closely agreed with observed EC throughout the simulation period [both during the soil evaporation (NDVI < 0.3) and transpiration dominant regimes (NDVI > 0.3)] (Fig. 3). This NDVI criterion is for visually differentiating (as indicated by symbol color) bare soil and the non-vegetated period from the vegetative period similar to Esau et al. (2016) and Qin et al. (2020). Evapotranspiration time series tended to follow the solar radiation and air temperature patterns where it mostly declined during the end of the year and gradually increased afterward (Fig. 3). The dominance of soil evaporation (E) during planting and the initial growing period (small  $f_c$ ) may also have contributed to this behavior. Due to multiple  $I_{rr}$

events, the growing period ET resembled the full canopy cover period indicating the importance of soil evaporation during the early growing period when reference ET was higher. As expected, large spikes in ET were observed after  $I_{rr}$  and P, mostly during the partial canopy cover period. BAITSSS was able to closely capture these wetting and drying events the majority of the time. In some instances, spikes observed by EC were missed. For instance, a sudden spike of ET on DOY 278 (Fig. 3h, YID 17b) was missed by BAITSSS where no  $I_{rr}$  or P was recorded during those days. This increase in ET was not supported by weather data. We suspected that the  $I_{rr}$  event on that day may have not been recorded due to a corresponding increase in soil moisture; however, EC was able to capture this. In a different instance in the same site, ET from BAITSSS showed a large spike around DOY 320 mostly due to transpiration (T), however, no such spike was recorded by EC (Fig. 3h). The partitioned ET from BAITSSS for YID 17c (Fig. 3i) showed evaporation (E) was dominant for the entire simulation period. As indicated earlier, this site not only had the lowest vegetation indices compared to other sites but also the vegetation indices significantly decreased after NDVI peak. Overall, BAITSSS was able to reasonably estimate ET for a wide range of soil moisture characteristics (Table 2) from low field capacity ( $0.19 \text{ m}^3 \text{ m}^{-3}$ ; NGIDD 19-20a and YID 19-20a) to high field capacity ( $0.42 \text{ m}^3 \text{ m}^{-3}$ ; YCWUA 18a and YCWUA 19-20a). However, it tended to slightly underestimate ET compared

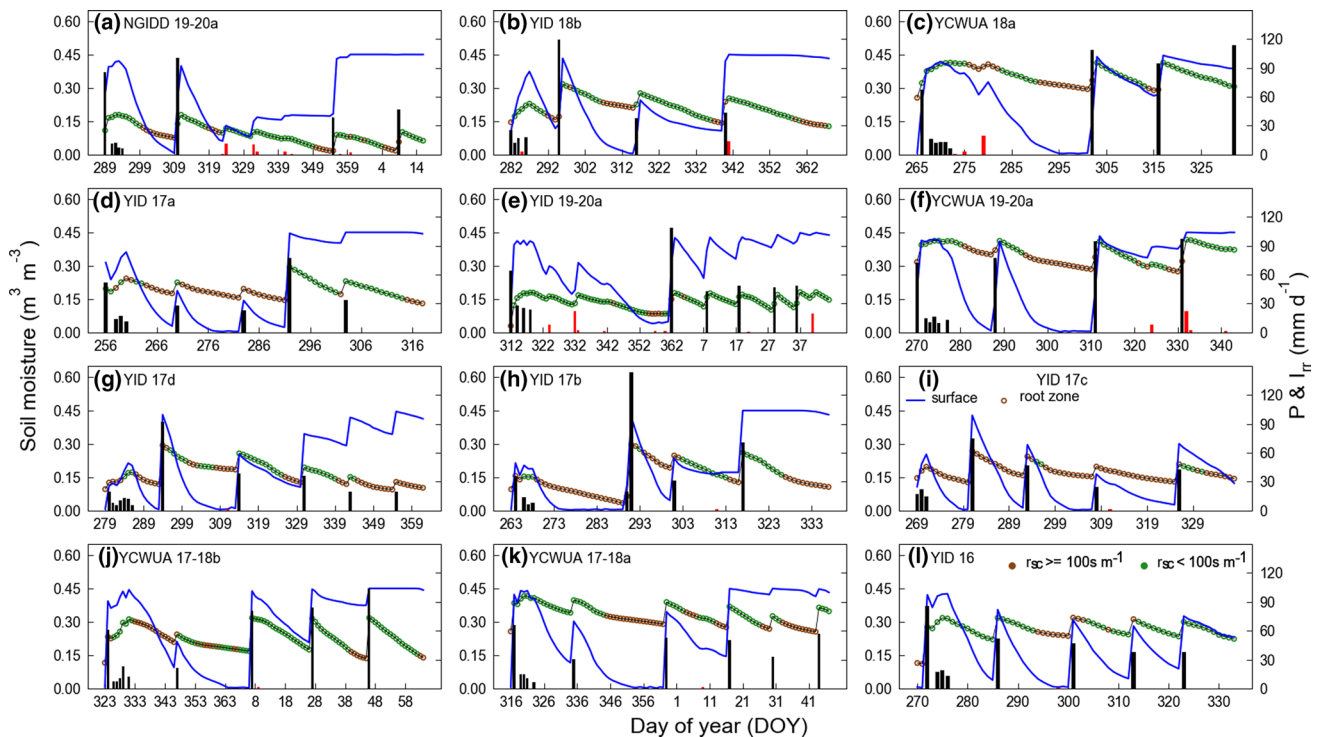


**Fig. 4** Estimated daily mean soil moisture at surface ( $\theta_{\text{sur}}$ , blue) and root zone ( $\theta_{\text{root}}$ , green or brown), applied irrigation, and precipitation of lettuce for various sites over multiple years (2016–2020) at Colo-

rado River Basin region. The  $\theta_{\text{root}}$  status is indicated by  $r_{\text{sc}}$  values less than  $100 \text{ s m}^{-1}$  for 6 or longer hours during that day (green) or otherwise coded in brown (color figure online)

to EC for certain time intervals during the simulation period (Fig. 3f, i). This may be because of the timing and duration of irrigation and precipitation events, soil moisture conditions, and intrinsic differences between the two methods. Evapotranspiration from EC for YCUWA 17–18a stayed relatively stable and showed minimal response to some irrigation events compared to BAITSSS after the new year (Fig. 3k). The ET spikes from BAITSSS were similar to EC at the start of the simulation in the majority of sites though some differences were observed in some sites (YID 17a, YID 17d). The maximum values of ET from EC and BAITSSS agreed closely within  $\sim 8.0 \text{ mm}$  during the simulation years. Results showed the timing accuracy of these applied  $I_{\text{tr}}$  and  $P$  events were critical to precisely capture these wetting and drying events and ultimately to estimate accurate ET values mostly in the partial canopy period.

Johnson and Trout (2012) found mean daily lettuce ET of  $2.1 \text{ mm}$  and maximum ET of  $3.4 \text{ mm}$  using satellite-based NDVI and reference ET for California's San Joaquin Valley. They found the daily ET uncertainty was less than  $0.5 \text{ mm}$  ( $0.31 \text{ mm}$  during development and  $0.16 \text{ mm}$  during mid-season) with total seasonal uncertainty of  $+10\%$  when compared to lysimeter-measured ET. The seasonal crop water consumption of lettuce ( $140 \text{ mm}$  to  $>400 \text{ mm}$ ) can vary based on climate types, irrigation methods, and crop management practices. For instance, the reported seasonal ET

of lettuce was  $\sim 145 \text{ mm}$  in Salinas Valley, California (Gallardo et al. 1996),  $\sim 200\text{--}300 \text{ mm}$  in Mesa, AZ (Erie et al. 1982), and from Monterey Bay, CA (Veihmeyer and Holland 1949), and  $>400 \text{ mm}$  in southern New Mexico (Sammis et al. 1988), and low California desert land (Turini et al. 2011). The estimated mean daily ET was  $3.4 \text{ mm}$  from EC and  $3.5 \text{ mm}$  from BAITSSS. Similarly, the mean seasonal ET was  $271 \text{ mm}$  from EC and  $278 \text{ mm}$  from BAITSSS. The estimated daily and seasonal ET of this study closely corresponded to the earlier studies.

### Soil moisture and resistances

Inverse, non-linear, relationships between soil moisture and resistances are the foundation of the resistance-based modeling schemes (i.e., large soil moisture related to small resistance and vice versa). These estimated soil moisture and resistance provided the means of estimating ET. The  $r_{\text{sc}}$  is affected by multiple factors ( $F_1, F_2, F_3,$  and  $F_4$ ) including  $\theta_{\text{root}}$  and varies on an hourly scale. During the nighttime,  $r_{\text{sc}}$  becomes large because of the lack of solar radiation ( $F_1$  becomes very small). The response of estimated soil moisture to applied  $I_{\text{tr}}$  and  $P$  is shown (Fig. 4), where the model predicted the large spikes at the surface ( $\theta_{\text{sur}}$ ) layer right after precipitation and irrigation. This response was because of the surface layer's position and a shallower depth compared



to the root zone, while this response was milder in the root zone. The  $\theta_{\text{sur}}$  increased to saturation while  $\theta_{\text{root}}$  was limited to the field capacity (Fig. 4). It was because the total available water (TAW) that can be extracted by the vegetation is computed between  $\theta_{\text{fc}}$  and  $\theta_{\text{wp}}$ . The  $\theta_{\text{sur}}$  rapidly declined after precipitation and irrigation events and reached the lower threshold and stayed low until the subsequent wetting events.

The color code (green) in  $\theta_{\text{root}}$  (Fig. 4) indicates the  $r_{\text{sc}}$  values lesser than  $100 \text{ sm}^{-1}$  for 6 or more hours during that day. The purpose was to differentiate between days and periods where the  $r_{\text{sc}}$  were small and large. In certain instances, when ET was underestimated by BAITSSS compared to EC (Fig. 3), it was evident that  $r_{\text{sc}}$  values were larger to those periods (brown color-coded). This underestimation might be related to the stomatal closure pointing to Jarvis parametrization of overestimation of soil moisture deficit as well as structural differences between EC and BAITSSS. Compared to other sites, YID 17c (Fig. 4i) showed relatively large  $r_{\text{sc}}$  ( $> 100 \text{ sm}^{-1}$ ) and small ET for the entire simulation. It was because of smaller vegetation indices than the rest of the sites which mostly reduced the transpiration (Fig. 3i). During the period where vegetation indices were significantly less than seasonal maxima, namely planting and early growth, variations in  $r_{\text{sc}}$  do not depend upon LAI or  $f_c$ , but are function of differences in soil hydraulic characteristics and initialization of  $\theta_{\text{wp}}$  at the start of the simulation. Indeed, the total contribution of transpiration to ET was negligible as  $f_c$  was small (Figs. 3 and 4). During that period, ET was mostly controlled by soil evaporation which in turn depends on soil moisture at the top layer and soil surface resistance ( $r_{\text{ss}}$ ). Soil evaporation showed some influence on  $\theta_{\text{root}}$  because the water balance at the root zone consists of both evaporation and transpiration and the adopted rooting depth of lettuce ( $\sim 500 \text{ mm}$ ) was comparably shallower than other grain crops ( $\sim 1000 \text{ mm}$ ).

### Cumulative evapotranspiration

The time series plot (Fig. 5) and bar plot (Fig. S1) showed the cumulative values of  $I_{\text{rr}}$ ,  $P$ , and ET where ET from BAITSSS closely followed the observed EC throughout the simulation period. The differences in the cumulative ET values (BAITSSS-EC) ranged from  $-14\%$  to  $25\%$  with a mean value of  $\sim 3\%$  (50% of sites had cumulative ET differences less than  $\sim 5\%$ ). Results showed that some sites had higher irrigation efficiency than others. For example, YID 18b (Fig. 5b) showed good agreement between BAITSSS and EC-observed ET as well as low differences between ET and applied water ( $I_{\text{rr}}$  plus  $P$ ) ( $\sim 15\%$ ) (Table 2). However, in YID 19-20a (Fig. 5e), applied water was  $\sim 40\%$  larger than the observed ET, and BAITSSS modeled ET showed good agreement with EC observations. Assessment of cumulative

totals showed ET from both methods mostly agreed irrespective of the significant differences in applied water among the sites (Fig. 5). These cumulative plots illustrate when applied  $I_{\text{rr}}$  diverged from ET. Additionally, some sites had larger cumulative ET during the period when evaporation was dominant ( $\text{NDVI} < 0.3$ ). The maximum cumulative ET from EC was  $314 \text{ mm}$  for NGIDD 19–20a and BAITSSS was  $381 \text{ mm}$  for YCWUA 17–18b, while the maximum value of applied  $I_{\text{rr}}$  was  $443 \text{ mm}$  for YCWUA 18a. Applied water was larger than ET in all sites (for both EC and BAITSSS) except for YID 17a and YID 17c where ET from EC was slightly larger. It may be because of random errors in either irrigation measurements/recording or EC measurements. For YCWUA 18a (Figs. 3c and 5c), more than  $100 \text{ mm}$   $I_{\text{rr}}$  was applied on the last day of the simulation, which created a large difference (44%) between applied water and ET from EC. The difference between the applied  $I_{\text{rr}}$  and ET will be reduced if this  $I_{\text{rr}}$  event was not included in the analysis.

### Statistical performance

Correlations between ET from BAITSSS and EC are shown in Fig. 6, with coefficients of determination ( $r^2$ ) ranging from 0.34 to 0.75 and root mean square errors (RMSE) of  $0.87\text{--}1.49 \text{ mm d}^{-1}$  with an average RMSE of  $1.1 \text{ mm d}^{-1}$ . Statistics depending on the NDVI range ( $< 0.3$ ,  $> = 0.3$ ) were shown in Table 2. The BAITSSS estimated ET values lie on both sides of the 1:1 line symmetrically both during partial and full cover period, thus showing low bias. Differences in BAITSSS and EC ET may have been contributed by multiple factors including intrinsic behavior of models as well as the estimated resistances from BAITSSS (soil surface and canopy resistances) differing EC. These resistances are difficult to measure, and observations are not readily available. YCWUA 17-18a showed the lowest  $r^2$  (0.34) with RMSE of  $1.23 \text{ mm d}^{-1}$  (Fig. 6k) and cumulative ET difference of 21% (Fig. 5k). The overall accuracy in these twelve study sites slightly decreased (both RMSE and  $r^2$ ) when compared to the earlier study (two seasons) of corn (2016) and sorghum (2014) with the lysimeter (RMSE =  $0.68 \text{ mm d}^{-1}$  and  $r^2 = 0.92$ ). Large weighing lysimeter-measured evapotranspiration (ET) is considered to be the most accurate (Evetts et al. 2012; Moorhead et al. 2019; Liu et al. 2019), nevertheless, it is not widely available. Eddy covariance systems are more available than lysimeters and easier to install in cooperating farmers' fields.

The residual ET bias analysis (observed – predicted) was conducted (Fig. 7) using the Pearson correlation coefficient. Residual analysis showed the bias was evenly distributed over the range (similar to Fig. 6) which were mostly positively related. The coefficient of correlation ( $r$ ) was weak ( $0.0 < r < 0.5$ ) for the majority of sites with the largest  $r$  value being 0.40 for YCWUA 18a (Fig. 7c).

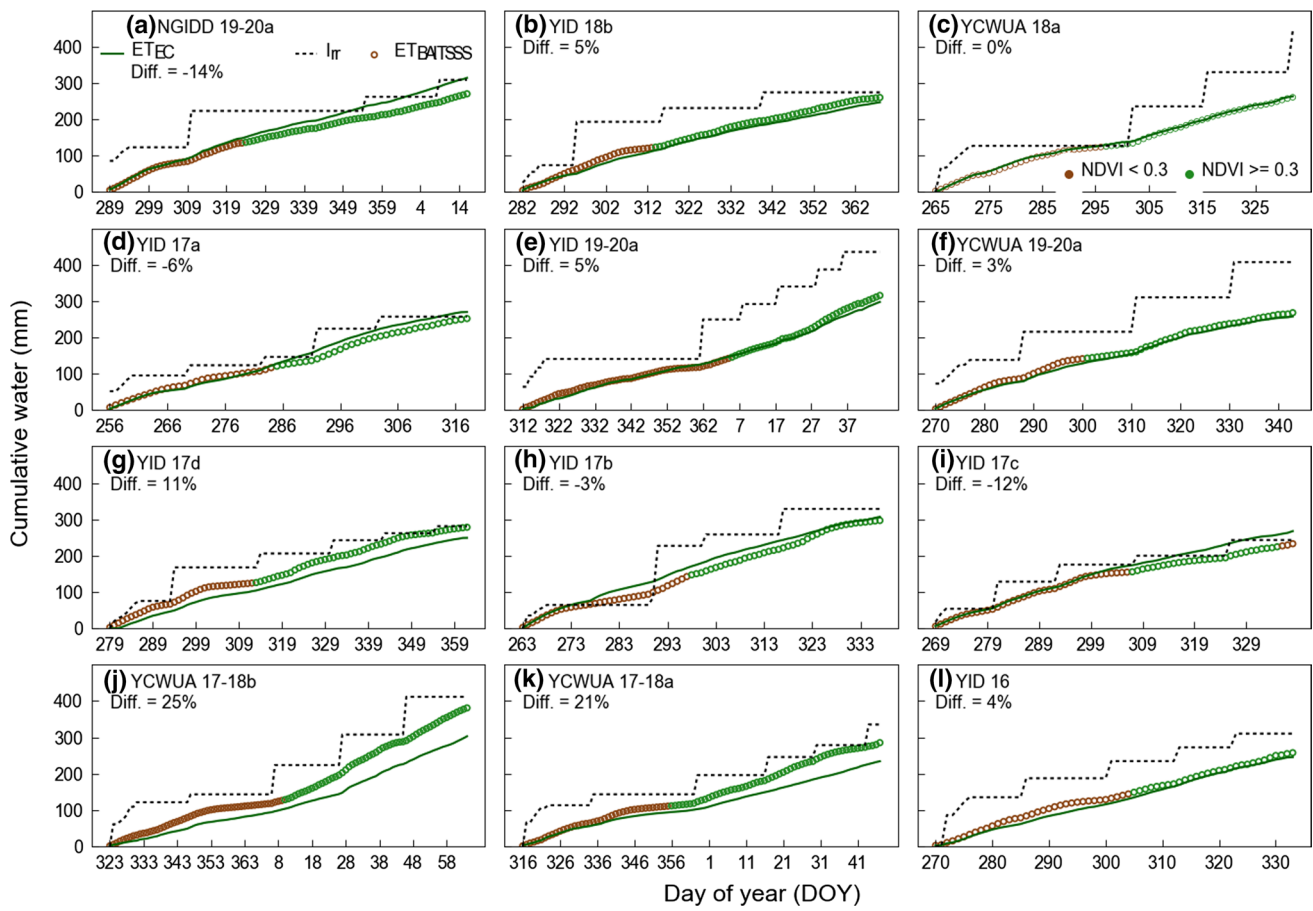


**Fig. 5** Cumulative water from EC, BAITSS, and applied irrigation of lettuce for various sites over multiple years (2016–2020) at Colorado River Basin region. ET varying on NDVI values indicated

by symbol color. Cumulative differences of ET between EC and BAITSS are shown in % (color figure online)

BAITSS needs information related to soil hydraulic characteristics, irrigation type, timing and amount, and rooting depth; such information may not be always available at the field level. As  $I_{rr}$  was mostly applied on the first day (or second) of the planting to all sites, analysis showed uncertainties related to the initial soil moisture boundary condition (soil moisture at root zone) were minimal when compared to EC (cumulative values, RMSE and  $r^2$ ). The analysis showed the assumption of  $\theta_{root}$  at field capacity at the start of simulation showed no significant difference from the assumption of wilting point. However, the assumptions of significantly smaller soil moisture at the root zone during the start of the simulation tended to underestimate ET to the sites with high field capacity. This underestimation was because the applied  $I_{rr}$  in the field was insufficient to have the soil moisture needed to avoid moisture-related stress in the Jarvis scheme. A root zone depth of 500 mm was able to reasonably mimic ET behavior. Significantly shallower rooting depth reduced ET during full cover due to the deficient soil moisture conditions in some sites. A larger rooting depth (> 500 mm) showed minimal impact on the final

ET as the model limits the  $R_{c\_min}$  with  $40 \text{ sm}^{-1}$  irrespective of soil moisture and energy available status. Overall, the analysis showed some influence of these factors on the final ET, however, fundamental model behavior remained intact. Comparison of hourly surface temperature between infrared thermometer (IRT) and derived by BAITSS was shown in Fig. S2 where BAITSS followed closely to IRT with some exceptions.

In an earlier study, sensitivity analysis was conducted from the BAITSS model to assess the accuracy of input parameters (weather and vegetation indices), where results showed parameter's accuracy affected the final ET (Dhungel et al. 2019b). There was about a 15% overestimation of ET using gridded input data (remote-sensing-based vegetation indices and gridded-based weather data) when compared to ground-based measured data.

The current study reaffirmed BAITSS being stable as a surface energy balance model and was effective for estimating ET of lettuce for an arid environment. It may be because of having the capability of accounting for the actual irrigation applied in the field. It showed a clear advantage of

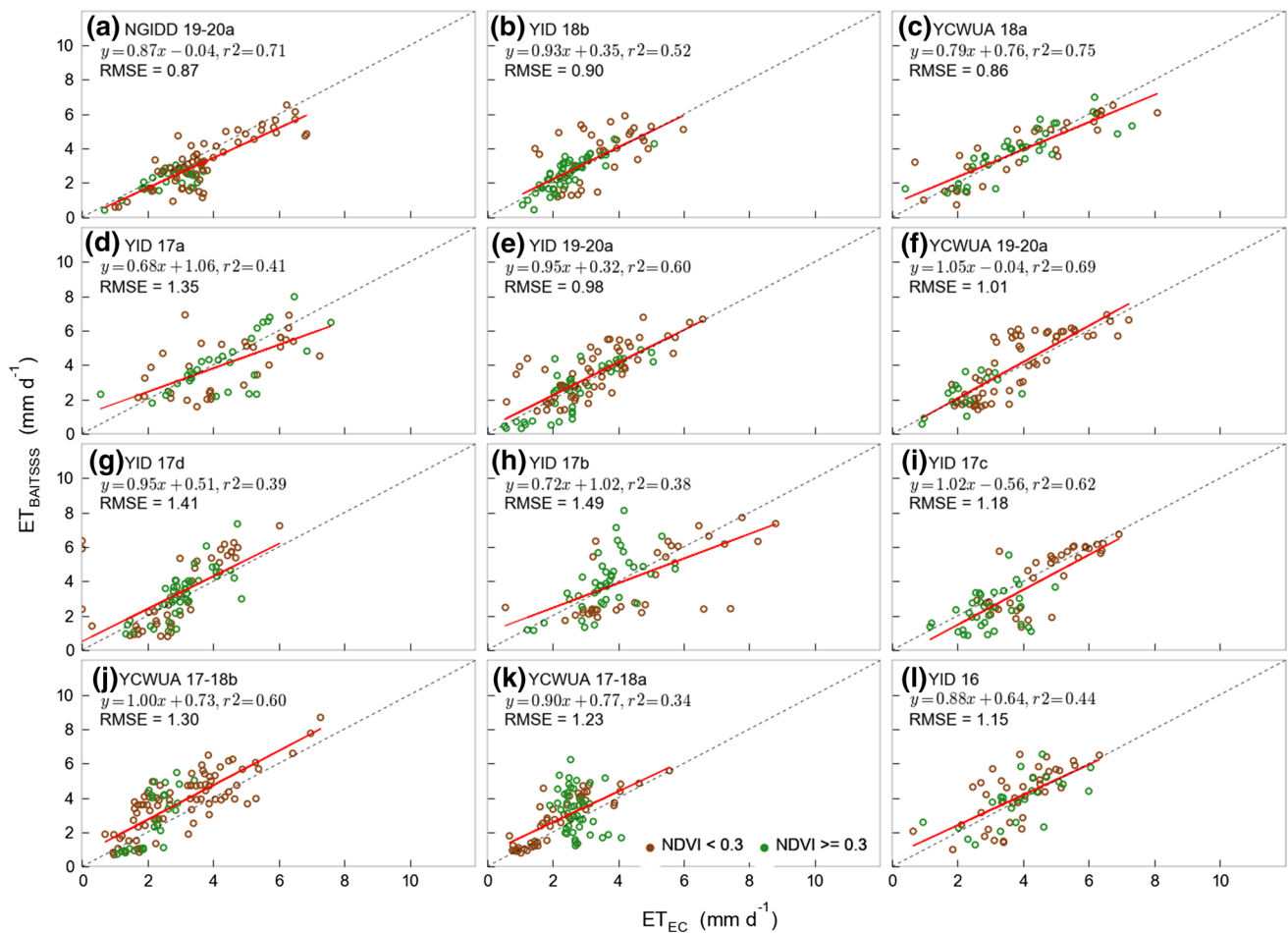


**Fig. 6** Scatterplots of daily evapotranspiration between BAITSSS and EC of lettuce for various sites over multiple years (2016–2020) at Colorado River Basin region. ET varying on NDVI values indicated

by symbol color; linear regression (red lines) and one-to-one correspondence (black dashed line) are also indicated (color figure online)

capturing the earlier period ET when fractional canopy cover was less, mostly when soil evaporation was dominant. During the full canopy period, both EC and BAITSSS closely agreed indicating the competence of the model during the period when soil radiation and air temperature were mostly declining. The minimum canopy resistance of  $40 \text{ sm}^{-1}$  utilized in the model was able to mimic ET estimated from EC.

## Conclusion

We evaluated ET from the BAITSSS model against twelve EC sites from 2016 to 2020 for vegetable crops (lettuce) grown in the arid environment of the Lower Colorado River Basin, USA for various soil moisture characteristics within several limitations (with no ground-based parameters such as soil moisture characteristics, fraction of canopy cover, etc.). Results showed  $I_{rr}$  application and effectiveness varied among the sites and within the identical soil hydraulic

characteristics. Differences in planting dates and length of simulation made it difficult to quantify the impact of these soil hydraulic characteristics on final ET. BAITSSS simulation showed some influence of initial soil moisture boundary conditions to the final ET depending on the soil hydraulic characteristics. However,  $I_{rr}$  at the start of the simulation (first or second day) minimized the impact of initial soil moisture boundary conditions. Mean cumulative ET differences between EC observations and model estimates were  $\sim 3\%$  among the sites while applied water was 30% larger in 33% of the sites. BAITSSS was able to estimate relatively accurate ET when compared to eddy covariance observations of ET for lettuce whose phenology and growing period are comparatively different from grain crops. The study highlighted the importance of soil water balance components in energy balance, and the timing and amount of  $I_{rr}$  to mimic the spikes and decrease of ET right after  $I_{rr}$ , especially during the growing period. Furthermore, the study demonstrated the capability of BAITSSS for estimating ET

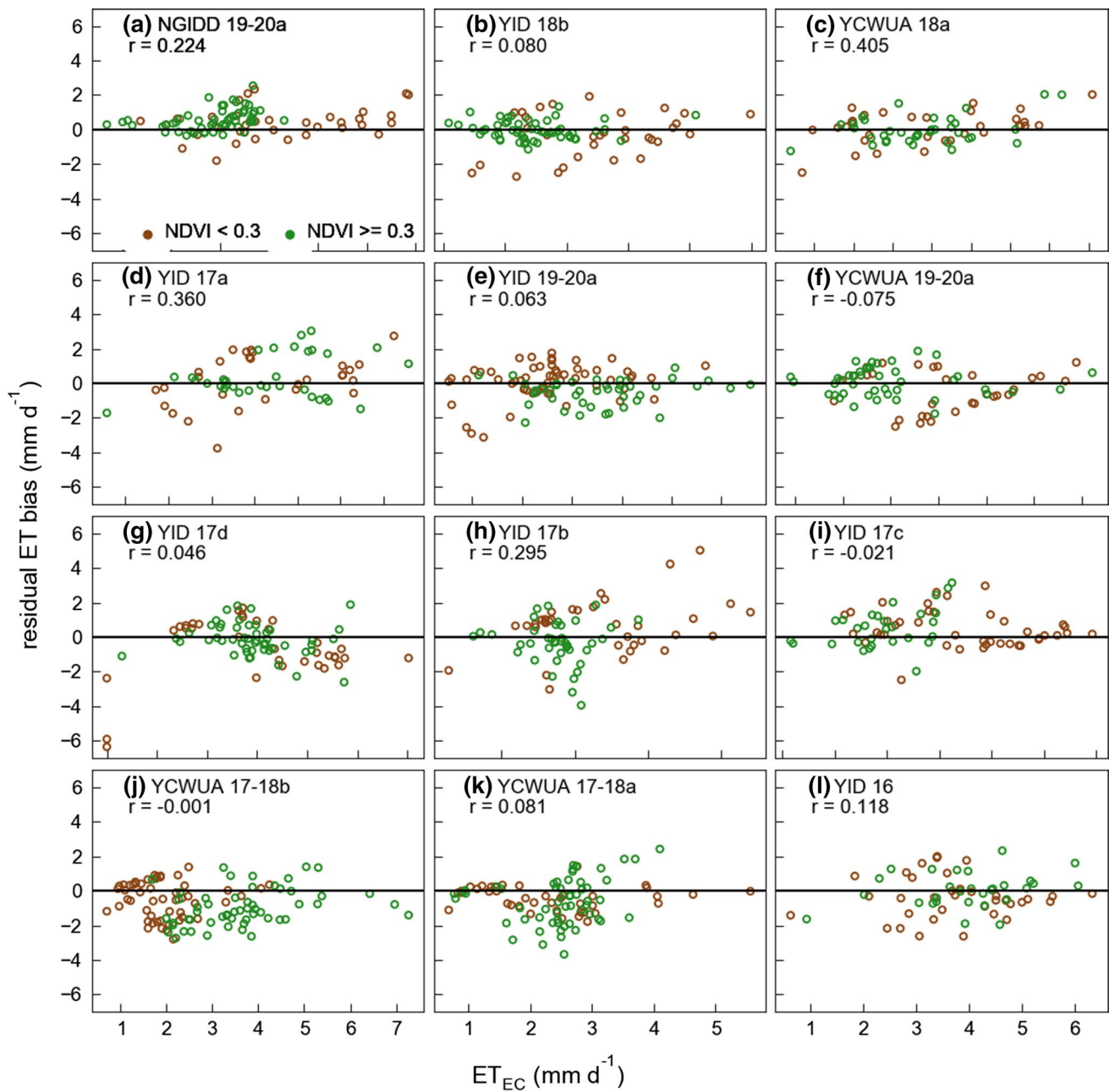


**Fig. 7** Daily residual bias plots of BAITSSS simulated ET on ET from EC (observed) of lettuce for various sites over multiple years (2016–2020) at Colorado River Basin region. ET varying on NDVI values indicated by symbol color (color figure online)

without directly relying on the thermal-based surface temperature. This intercomparison also indicates the usefulness and transferability of the model in data-limited conditions. Comparison of modeled E and T to observations (from flux variance partitioning of ET, microlysimeters, and other approaches) can help to identify the biases in ET if any. Availability of measured data (soil hydraulic characteristics, vegetation indices) and boundary conditions (soil moisture at the beginning and during simulation) will help to further

understand and evaluate their role and can help to increase model accuracy.

**Supplementary Information** The online version contains supplementary material available at <https://doi.org/10.1007/s00271-022-00814-x>.

**Acknowledgements** This work is supported by Agriculture and Food Research Initiative Competitive Grant no. 2020-69012-31914 from the USDA National Institute of Food and Agriculture. This research was supported in part by the U.S. Department of Agriculture, Agricultural Research Service (project numbers 2036-61000-018-000-D

and 2020-13660-008-000-D). This research used resources provided by the SCINet project of the USDA Agricultural Research Service, ARS project number 0500-00093-001-00-D. The U.S. Department of Agriculture prohibits discrimination in all its programs and activities on the basis of race, color, national origin, age, disability, and where applicable, sex, marital status, familial status, parental status, religion, sexual orientation, genetic information, political beliefs, reprisal, or because all or part of an individual's income is derived from any public assistance program. (Not all prohibited bases apply to all programs.) Persons with disabilities who require alternative means for communication of program information (Braille, large print, audiotape, etc.) should contact USDA's TARGET Center at (202) 720-2600 (voice and TDD). To file a complaint of discrimination, write to USDA, Director, Office of Civil Rights, 1400 Independence Avenue, S.W., Washington, D.C. 20250-9410, or call (800) 795-3272 (voice) or (202) 720-6382 (TDD). USDA is an equal opportunity provider and employer.

**Author contributions** R.D, R.G.A, and A.F. designed and performed research, analyzed data, and originated manuscript; M.S. and C.A.S. contributed data; E.S. guided project development. All authors reviewed and revised the manuscript.

## Declarations

**Conflict of interests** The authors declare no conflicts of interest relevant to this study.

## References

- Alexandridis TK, Panagopoulos A, Galanis G et al (2014) Combining remotely sensed surface energy fluxes and GIS analysis of groundwater parameters for irrigation system assessment. *Irrig Sci* 32:127–140. <https://doi.org/10.1007/s00271-013-0419-8>
- Allen RG, Pereira LS, Raes D, Smith M (1998) Crop evapotranspiration-guidelines for computing crop water requirements-FAO Irrigation and drainage paper 56. Fao, Rome 300:D05109
- Allen RG, Pereira LS, Smith M et al (2005a) *FAO-56* dual crop coefficient method for estimating evaporation from soil and application extensions. *J Irrig Drain Eng* 131:2–13. [https://doi.org/10.1061/\(ASCE\)0733-9437\(2005\)131:1\(2\)](https://doi.org/10.1061/(ASCE)0733-9437(2005)131:1(2))
- Allen RG, Walter IA, Elliot R, et al (2005b) The ASCE standardized reference evapotranspiration equation. ASCE-EWRI task committee final report
- Anderson RG, Wang D (2014) Energy budget closure observed in paired Eddy Covariance towers with increased and continuous daily turbulence. *Agric Forest Meteorol* 184:204–209
- Anderson MC, Yang Y, Xue J et al (2021) Interoperability of ECOSTRESS and Landsat for mapping evapotranspiration time series at sub-field scales. *Remote Sens Environ* 252:112189. <https://doi.org/10.1016/j.rse.2020.112189>
- Anderson MC, Norman JM, Mecikalski JR et al (2007) A climatological study of evapotranspiration and moisture stress across the continental United States based on thermal remote sensing: 1. Model formulation: evapotranspiration and moisture stress. *J Geophys Res*. <https://doi.org/10.1029/2006JD007506>
- Arguez A, Durre I, Applequist S, et al (2010) U.S. Climate Normals Product Suite (1981–2010)
- Ball JT, Woodrow IE, Berry JA (1987) A Model Predicting Stomatal Conductance and its Contribution to the Control of Photosynthesis under Different Environmental Conditions. In: Biggins J (ed) *Progress in Photosynthesis Research*. Springer, Netherlands, pp 221–224
- Berardy A, Chester MV (2017) Climate change vulnerability in the food, energy, and water nexus: concerns for agricultural production in Arizona and its urban export supply. *Environ Res Lett* 12:035004. <https://doi.org/10.1088/1748-9326/aa5e6d>
- Bohn TJ, Vivoni ER (2016) Process-based characterization of evapotranspiration sources over the North American monsoon region. *Water Resour Res* 52:358–384. <https://doi.org/10.1002/2015WR017934>
- Chikamoto Y, Wang S-YS, Yost M et al (2020) Colorado River water supply is predictable on multi-year timescales owing to long-term ocean memory. *Commun Earth Environ* 1:26. <https://doi.org/10.1038/s43247-020-00027-0>
- Dhangel R, Allen RG, Trezza R, Robison CW (2016) Evapotranspiration between satellite overpasses: methodology and case study in agricultural dominant semi-arid areas: Time integration of evapotranspiration. *Met Apps* 23:714–730. <https://doi.org/10.1002/met.1596>
- Dhangel R, Aiken R, Colaizzi PD et al (2019a) Evaluation of uncalibrated energy balance model (BAITSSS) for estimating evapotranspiration in a semiarid, advective climate. *Hydrol Process* 33:2110–2130. <https://doi.org/10.1002/hyp.13458>
- Dhangel R, Aiken R, Colaizzi PD et al (2019b) Increased bias in evapotranspiration modeling due to weather and vegetation indices data sources. *Agron J* 111:1407–1424. <https://doi.org/10.2134/agronj2018.10.0636>
- Dhangel R, Aiken R, Evett SR et al (2021) Energy imbalance and evapotranspiration hysteresis under an advective environment: evidence from lysimeter, Eddy covariance, and energy balance modeling. *Geophys Res Lett*. <https://doi.org/10.1029/2020GL091203>
- Erie LJ, French OF, Bucks DA, Harris K (1982) *Consumptive Use of Water by Major Crops in the Southwestern United States*
- Esau I, Miles VV, Davy R et al (2016) Trends in normalized difference vegetation index (NDVI) associated with urban development in northern West Siberia. *Atmos Chem Phys* 16:9563–9577. <https://doi.org/10.5194/acp-16-9563-2016>
- Escarabajal-Henarejos D, Molina-Martínez JM, Fernández-Pacheco DG, García-Mateos G (2015) Methodology for obtaining prediction models of the root depth of lettuce for its application in irrigation automation. *Agric Water Manag* 151:167–173. <https://doi.org/10.1016/j.agwat.2014.10.012>
- Evett SR, Schwartz RC, Howell TA et al (2012) Can weighing lysimeter ET represent surrounding field ET well enough to test flux station measurements of daily and sub-daily ET? *Adv Water Resour* 50:79–90. <https://doi.org/10.1016/j.advwatres.2012.07.023>
- Falge E, Baldocchi D, Olson R et al (2001) Gap filling strategies for long term energy flux data sets. *Agric for Meteorol* 107:71–77. [https://doi.org/10.1016/S0168-1923\(00\)00235-5](https://doi.org/10.1016/S0168-1923(00)00235-5)
- Fisher JB, Melton F, Middleton E et al (2017) The future of evapotranspiration: Global requirements for ecosystem functioning, carbon and climate feedbacks, agricultural management, and water resources: The future of evapotranspiration. *Water Resour Res* 53:2618–2626. <https://doi.org/10.1002/2016WR020175>
- Fratini G, Mauder M (2014) Towards a consistent eddy-covariance processing: an intercomparison of EddyPro and TK3. *Atmos Measur Techn* 7:2273–2281
- French AN, Hunsaker DJ, Sanchez CA et al (2020) Satellite-based NDVI crop coefficients and evapotranspiration with eddy covariance validation for multiple durum wheat fields in the US Southwest. *Agric Water Manag* 239:106266. <https://doi.org/10.1016/j.agwat.2020.106266>
- Frisvold G, Sanchez C, Gollehon N et al (2018) Evaluating gravity-flow irrigation with lessons from Yuma, Arizona, USA. *Sustainability* 10:1548. <https://doi.org/10.3390/su10051548>

- Gallardo M, Snyder RL, Schulbach K, Jackson LE (1996) Crop growth and water use model for Lettuce. *J Irrig Drain Eng* 122:354–359. [https://doi.org/10.1061/\(ASCE\)0733-9437\(1996\)122:6\(354\)](https://doi.org/10.1061/(ASCE)0733-9437(1996)122:6(354))
- Gutman G, Ignatov A (1998) The derivation of the green vegetation fraction from NOAA/AVHRR data for use in numerical weather prediction models. *Int J Remote Sens* 19:1533–1543. <https://doi.org/10.1080/014311698215333>
- He R, Jin Y, Kandelous M et al (2017) Evapotranspiration estimate over an almond Orchard using landsat satellite observations. *Remote Sensing* 9:436. <https://doi.org/10.3390/rs9050436>
- Jarvis PG (1976) The interpretation of the variations in leaf water potential and stomatal conductance found in canopies in the field. *Phil Trans R Soc Lond B* 273:593–610. <https://doi.org/10.1098/rstb.1976.0035>
- Johnson LF, Trout TJ (2012) Satellite NDVI assisted monitoring of vegetable crop evapotranspiration in California's San Joaquin valley. *Remote Sensing* 4:439–455. <https://doi.org/10.3390/rs4020439>
- Johnson LF, Cahn M, Martin F et al (2016) Evapotranspiration-based irrigation scheduling of head lettuce and broccoli. *HortScience* 51:935–940
- Kilic A, Allen R, Trezza R et al (2016) Sensitivity of evapotranspiration retrievals from the METRIC processing algorithm to improved radiometric resolution of Landsat 8 thermal data and to calibration bias in Landsat 7 and 8 surface temperature. *Remote Sens Environ* 185:198–209. <https://doi.org/10.1016/j.rse.2016.07.011>
- Kljun N, Calanca P, Rotach MW, Schmid HP (2015) A simple two-dimensional parameterisation for Flux Footprint Prediction (FFP). *Geoscient Model Develop* 8:3695–3713. <https://doi.org/10.5194/gmd-8-3695-2015>
- Kumar A, Chen F, Niyogi D et al (2011) Evaluation of a photosynthesis-based Canopy resistance formulation in the Noah Land-surface model. *Boundary-Layer Meteorol* 138:263–284. <https://doi.org/10.1007/s10546-010-9559-z>
- Leuning R (1990) Modelling stomatal behaviour and photosynthesis of eucalyptus grandis. *Function Plant Biol* 17:159. <https://doi.org/10.1071/PP9900159>
- Leuning R (1995) A critical appraisal of a combined stomatal-photosynthesis model for C3 plants. *Plant Cell Environ* 18:339–355. <https://doi.org/10.1111/j.1365-3040.1995.tb00370.x>
- Leuning R, van Gorsel E, Massman WJ, Isaac PR (2012) Reflections on the surface energy imbalance problem. *Agric Forest Meteorol* 156:65–74. <https://doi.org/10.1016/j.agrformet.2011.12.002>
- Lhomme J-P, Elguero E, Chehbouni A, Boulet G (1998) Stomatal control of transpiration: Examination of Monteith's formulation of canopy resistance. *Water Resour Res* 34:2301–2308. <https://doi.org/10.1029/98WR01339>
- Liu B, Cui Y, Shi Y et al (2019) Comparison of evapotranspiration measurements between eddy covariance and lysimeters in paddy fields under alternate wetting and drying irrigation. *Paddy Water Environ* 17:725–739. <https://doi.org/10.1007/s10333-019-00753-y>
- Long D, Singh VP (2010) Integration of the GG model with SEBAL to produce time series of evapotranspiration of high spatial resolution at watershed scales. *J Geophys Res* 115:D21128. <https://doi.org/10.1029/2010JD014092>
- Lund J, Medellin-Azuara J, Durand J, Stone K (2018) Lessons from California's 2012–2016 drought. *J Water Resour Plann Manage* 144:04018067. [https://doi.org/10.1061/\(ASCE\)WR.1943-5452.0000984](https://doi.org/10.1061/(ASCE)WR.1943-5452.0000984)
- Massari C, Modanesi S, Dari J et al (2021) A review of irrigation information retrievals from space and their utility for users. *Remote Sensing* 13:4112. <https://doi.org/10.3390/rs13204112>
- Melton FS, Johnson LF, Lund CP et al (2012) Satellite irrigation management support with the terrestrial observation and prediction system: a framework for integration of satellite and surface observations to support improvements in agricultural water resource management. *IEEE J Sel Top Appl Earth Observ Remote Sensing* 5:1709–1721. <https://doi.org/10.1109/JSTARS.2012.2214474>
- Melton FS, Huntington J, Grimm R et al (2021) OpenET: filling a critical data gap in water management for the western United States. *J Am Water Resour Assoc* 1752–1688:12956. <https://doi.org/10.1111/1752-1688.12956>
- Moorhead J, Marek G, Gowda P et al (2019) Evaluation of evapotranspiration from eddy covariance using large weighing Lysimeters. *Agronomy* 9:99. <https://doi.org/10.3390/agronomy9020099>
- Norton CL, Dannenberg MP, Yan D et al (2021) Climate and socioeconomic factors drive irrigated agriculture dynamics in the lower Colorado river basin. *Remote Sensing* 13:1659. <https://doi.org/10.3390/rs13091659>
- Qin B, Cao B, Li H et al (2020) Evaluation of six high-spatial resolution clear-sky surface upward longwave radiation estimation methods with MODIS. *Remote Sensing* 12:1834. <https://doi.org/10.3390/rs12111834>
- Reichstein M, Falge E, Baldocchi D et al (2005) On the separation of net ecosystem exchange into assimilation and ecosystem respiration: review and improved algorithm. *Glob Change Biol* 11:1424–1439. <https://doi.org/10.1111/j.1365-2486.2005.001002.x>
- Rosa R, Tanny J (2015) Surface renewal and eddy covariance measurements of sensible and latent heat fluxes of cotton during two growing seasons. *Biosys Eng* 136:149–161. <https://doi.org/10.1016/j.biosystemseng.2015.05.012>
- Roux B, van der Laan M, Vahrmeijer T et al (2016) Estimating water footprints of vegetable crops: influence of growing season, solar radiation data and functional unit. *Water* 8:473. <https://doi.org/10.3390/w8100473>
- Sammis TW, Kratky BA, Wu IP (1988) Effects of limited irrigation on lettuce and Chinese cabbage yields. *Irrig Sci*. <https://doi.org/10.1007/BF00275431>
- Sanchez CA, Zerihun D, Farrell-Poe KL (2009) Management guidelines for efficient irrigation of vegetables using closed-end level furrows. *Agric Water Manag* 96:43–52. <https://doi.org/10.1016/j.agwat.2008.06.010>
- Shu FS (1982) Moisture and heat transport in a soil layer forced by atmospheric conditions. M.Sc Thesis, Univ of Connecticut
- Thorup-Kristensen K (2001) Root growth and soil nitrogen depletion by onion, lettuce, early cabbage and carrot. *Acta Hort*. <https://doi.org/10.17660/ActaHortic.2001.563.25>
- Turini T, Cahn M, Cantwell M et al (2011). Iceberg Lettuce Production in California. <https://doi.org/10.3733/ucanr.7215>
- Veihmeyer FJ, Holland AH (1949) Irrigation and cultivation of lettuce
- Vickers D, Mahrt L (1997) Quality control and flux sampling problems for tower and aircraft data. *J Atmos Oceanic Tech* 14:512–526
- Webb EK, Pearman GI, Leuning R (1980) Correction of flux measurements for density effects due to heat and water vapour transfer. *Q J R Meteorol Soc* 106:85–100
- Wieczorek M (2014) Area-and depth-weighted averages of selected SSURGO variables for the conterminous United States and District of Columbia. US Geological Survey
- Zhang G, Zhou G, Chen F, Wang Y (2014) Analysis of the variability of canopy resistance over a desert steppe site in Inner Mongolia, China. *Adv Atmos Sci* 31:681–692. <https://doi.org/10.1007/s00376-013-3071-6>

**Publisher's Note** Springer Nature remains neutral with regard to jurisdictional claims in published maps and institutional affiliations.